PAPER • OPEN ACCESS

Space charge compensation of positive ion beams used in magnetic fusion applications

To cite this article: A.J.T. Holmes and R. McAdams 2022 *Nucl. Fusion* **62** 066017

OPEN ACCESS
IOP Publishing | International Atomic Energy Agency Nuclear Fusion
Nucl. Fusion **62** (2022) 066017 (15pp) https://doi.org/10.1088/1741-4326/ac544c

Space charge compensation of positive ion beams used in magnetic fusion applications

A.J.T. Holmes[1] **and R. McAdams**[2,*]

[1] Marcham Scientific, Hungerford, Berkshire RG17 0LH, United Kingdom
[2] United Kingdom Atomic Energy Authority, Culham Centre for Fusion Energy, Culham Science Centre, Abingdon, Oxon, OX14 3DB, United Kingdom

E-mail: roy.mcadams@ukaea.uk

Received 25 October 2021, revised 27 January 2022
Accepted for publication 10 February 2022
Published 5 April 2022

Abstract

A model is presented for space charge neutralisation of positive ion beams. The model is used for the particular case of the beams used for magnetic based fusion applications. The beams consist, after a gas neutraliser, of ions and atoms at different energies. Account is taken of the contribution of all beam components to ionization of the background gas. Consideration is also given to not only beam heating of the plasma generated by the beam, due to Coulomb collisions, but also to Coulomb heating by fast electrons produced in ionization by all beam particles and stripping of the neutral components. Two approximations are considered for the motion of the secondary ions out of the beam potential; a drift approximation and a freefall approximation. All the beam plasma parameters can be calculated. The model is applied to a typical extracted beam of deuterium ions of 120 kV, 60 A. It is found that these beams are very highly compensated and that beam plasma heating by the electrons produced is generally greater than that due to the beam ions.

Keywords: neutral beam injection, space charge compensation, positive ion beam

(Some figures may appear in colour only in the online journal)

1. Introduction

Neutral beams of atoms and molecules used in magnetic fusion applications for heating, current drive and diagnostics are produced from an ion beam from an accelerator passing through a gas neutraliser cell. The resulting beam is a mixture of residual ion, atoms and molecules. The residual ions are removed from the composite beam usually by a magnetic field and the neutral beam then drifts into the plasma device such as a tokamak.

A charged particle beam is subject to two internal forces arising from interactions between the particles. Firstly there is a repulsive force due to the Coulombic interaction between the like charges in the beam. Secondly there is an attractive force due to the magnetic fields arising from the moving charges. For a non-relativistic beam the ratio of the magnitudes of the magnetic to electric forces is β^2 [1] where $\beta = v_b/c$ and v_b is the beam velocity and c is the velocity of light. For applications such as producing neutral beams of atoms and molecules for controlled magnetic fusion on devices such as the Joint European Torus (JET) indicative precursor beams of 60 A, 120 kV D^+ are used [2]. Such a beam is non-relativistic and the magnetic force can be ignored. The potential across the beam from the centre to the beam edge for a uniform distribution of ions is $I/4\pi\varepsilon_0 v_b$ where I is the beam current and ε_0 is the permittivity of free space. For such a beam this potential is ~158 kV and if this repulsion is unmitigated the beam cannot travel any significant distance. Space charge effects could thus affect the transmission of the beam into the fusion device and the trajectories of residual ions removed from the beam in

* Author to whom any correspondence should be addressed.

order to produce a neutral beam for injection into the fusion device.

The mitigation of the repulsive space charge force is known as space charge compensation or neutralisation. The beam passes through a background gas and forms a plasma consisting of the beam ions, secondary slow ions and electrons causing by collisions with the gas. Ionisation and charge exchange give rise to the slow ions and electrons e.g. for a D^+ beam for example

$$\underline{D}^+ + D_2 \rightarrow \underline{D}^+ + {D_2}^+ + \text{e ionization}$$

$$\underline{D}^+ + D_2 \rightarrow \underline{D} + {D_2}^+ \text{ charge exchange.}$$

The ejected electrons may also ionize the background gas. The slow ions are expelled from the beam due to the positive potential. The electrons remain in the beam unless they have sufficient energy to escape. The overall beam potential is thus reduced and the beam can then move with much reduced divergence compared to the uncompensated beam case.

Space charge compensation has been studied extensively by Gabovich and Solosochenko and co-workers; see the reviews [3, 4] for example. Soloschenko [4] developed an expression for the compensated potential of the beam. The approach was to balance the energy required for the electrons to leave the beam with that derived from heating by the beam itself. The resulting expression for the compensated beam potential involved two terms. One term is dominant at low pressure and does not involve the motion of the secondary ions whereas the second terms is dominant at higher pressures and involves an average velocity for the secondary ions and also depends on the size of the beam. Winklehner *et al* [5] measured the beam potential for Ar^{8+} and O^{6+} beams and found good agreement with this model if an ion temperature was chosen close to the value of the beam potential. This model does not allow for the electron temperature or the plasma densities to be determined.

Holmes [6] was able to close the equations fully to determine the potential, plasma densities and temperature using continuity equations for the ions and electrons and the overall energy balance. Solving the continuity equation fully to give the radial density of ions taking into account the creation of ions at different radial positions and assuming the ions were in freefall in the potential from where they were created to the beam edge led to parabolic dependence of the potential on radius at small radii. Given the freefall nature of the movement of the ions this model is essentially only applicable at low pressures or to small beams.

This paper will only address the situation for an intense multiple aperture beam in deuterium (or hydrogen if the ion and gas masses are changed) with particular relevance to neutral beam injection for thermonuclear fusion. Such beams are only created in a neutral beam injector where the beam has both a high current and beam kinetic energy and where the only background gas of any significance is the operating gas of the beam source (and neutralizer) which is the same as the beam itself. Other gases such as nitrogen or oxygen or water vapour are excluded as in the case examined here the very large pumping speed (10^6 l s^{-1}) makes these gas components negligible. Beams in other gases could be examined by changing the various cross-sections or rates used in the model but this is beyond the scope of this paper.

In this paper a model of space charge compensation in beams such as those used for magnetic fusion applications is presented. A basic model is developed and applied under two approximations. In the freefall approximation the secondary ions move out of the beam solely under the potential between where they are created and the edge of the beam. Such a model is applicable to small beams or low pressures in the beam path. In the drift approximation the secondary ions move with a velocity determined by their collisions with the background gas. This model might be expected to be more applicable to large beams and high beamline pressures where the mean free path is smaller than the beam dimension. The equations are solved not only to give the beam potential but also the plasma electron temperature and densities.

In all of the work described so far [3, 4, 6] it is assumed that the heating of the plasma electrons arises due to Coulomb collisions between these electrons and the beam ions. In this paper it is argued that the source of the heating is not from the beam ions alone but from the energy of the electrons ejected in forming the secondary ions. Their role in producing secondary electrons is also taken into account since it will be shown that their energy is sufficiently high.

In section 2, the properties of the beams used in magnetic fusion applications are described briefly. In section 3 the basic space charge neutralisation model is developed and then used in section 4 in the freefall and drift approximations. The method for solving the resultant equations is also outlined. The results from applying the model to a 120 kV, 60 A deuterium beam typical of that used on JET are discussed in section 5 and some conclusions are drawn in section 6.

2. Ion beams for magnetic fusion applications

Beams of fast atoms and molecules are used in magnetic fusion devices for heating the plasma, diagnostics and current drive. They must be neutral to avoid interaction with the magnetic field of the fusion machine used to confine the plasma. These beams are derived by extraction of an ion beam from a source, passing this beam through a gas cell or neutraliser to produce neutral components. The neutralisation is not 100% efficient and residual ions are swept out of the composite beam of ions and neutrals by a magnetic field. The neutral beam is then injected into the fusion device.

The JET machine uses positive ion beams of primarily deuterium but also tritium and hydrogen [2]. Taking the deuterium beam as an example, D^+, ${D_2}^+$ and ${D_3}^+$ ions are extracted from a magnetic multipole source. At high power the total extracted current is ~60 A and this is accelerated in a triode accelerator to 120 kV. The flux fractions of the D^+, ${D_2}^+$ and ${D_3}^+$ ions, $f_1{:}f_2{:}f_3$ are ~0.72:0.22:0.06. The neutraliser contains the same gas species as the ion source. The efficiency of the gas neutraliser for these beam parameters at the operating filling

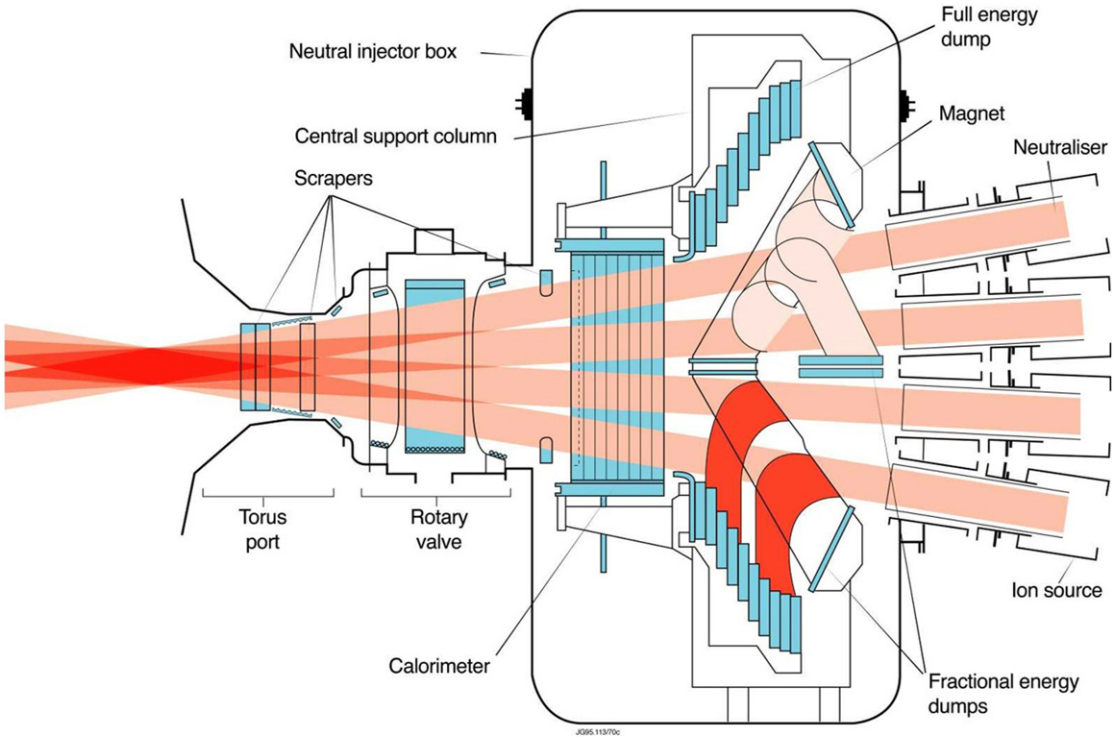

Figure 1. Elevation view of a JET Neutral Beam Injector box.

pressure is measured as ∼42%. Taking into account transmission and other losses the injected neutral beam power from the injector is just over 2 MW. JET has sixteen such injectors giving a total injected power capability of over 32 MW. An elevation view of the one of the two JET Neutral Beam Injector boxes consisting of eight injectors is shown in figure 1. It shows the ion source and neutralizer and the ion and neutral beam drifting to the magnet region, The residual ions are removed by the magnetic field and dumped. The neutral particles travel past a calorimeter through an isolating valve region and on into the tokamak plasma.

After exiting the neutraliser the composite beam has fourteen components arising from the interaction of the three extracted species with the gas in the neutraliser. The nine ion components are $D^+(E_b)$, $D^-(E_b)$, $D_2{}^+(E_b)$, $D^+(E_b/2)$, $D^-(E_b/2)$, $D_3{}^+(E_b)$, $D_2{}^+(2E_b/3)$, $D^+(E_b/3)$, and $D^-(E_b/3)$. The five neutral components are $D(E_b)$, $D_2(E_b)$, $D(E_b/2)$, $D_2(2E_b/3)$, and $D(E_b/3)$. E_b is the full beam energy determined by the accelerator voltage and the value in brackets is the particle energy. This paper does not deal with the space charge effects within the neutraliser as the fractions of the components are changing as the beam travels through the gas; the space charge compensation of the composite beam after the neutraliser will be modelled. The fractions depend on the neutralizer target thickness and this is dealt with below. Both the ionic and neutral components can contribute to the processes giving rise to space charge neutralisation e.g. all components can ionize the background gas creating secondary ions and electrons and the neutrals can be stripped to create further electrons. This is a lot to deal with.

The situation can be simplified because for an infinitely thick neutraliser target, the only remaining ion components are $D^+(E_b)$, $D^+(E_b/2)$, and $D^+(E_b/3)$ and the remaining neutral components are $D(E_b)$, $D(E_b/2)$, and $D(E_b/3)$ as these fractions have reached an equilibrium value. The kinetic energy of the component is shown in the brackets. These are the eventual products of the initial D^+, $D_2{}^+$ and $D_3{}^+$ ions. In the case of the JET injector operating parameters the 42% neutralisation corresponds to a target thickness of $\sim 5.5 \times 10^{19}$ m^{-2}. At this target thickness the three ionic components above comprise ∼95% of the residual ion beam power and the neutral components are also ∼95% of the neutral beam power. Hence it is a reasonable approximation to assume the beam is only made up of those six components.

The equilibrium fractions for the three neutral components $D(E_b)$, $D(E_b/2)$, and $D(E_b/3)$ are $F(E_b)$, $F(E_b/2)$, and $F(E_b/3)$ such that the equilibrium neutral fractions of the extracted power are $f_1{}^*F(E_b)$, $f_2{}^*F(E_b/2)$, $f_3{}^*F(E_b/3)$ respectively. The equilibrium fraction F only depends on various cross-sections for the processes in the neutraliser and values are found in various databases. Similarly, the fractions of the extracted power in the residual ions are $f_1{}^*(1 - F(E_b))$, $f_2{}^*(1 - F(E_b/2))$, $f_3{}^*(1 - F(E_b/3))$ respectively. A more concise notation for $F(E_b)$, $F(E_b/2)$, and $F(E_b/3)$ of F_1, F_2 and F_3 respectively will be used in the remainder of this paper.

The general model will apply to the region between the exit of the neutraliser and the bend magnet. Space charge effects in his region and indeed in the neutraliser could affect the beam divergence and hence the transmission into the machine. However, the model is general enough to consider the ion components alone beyond the magnet.

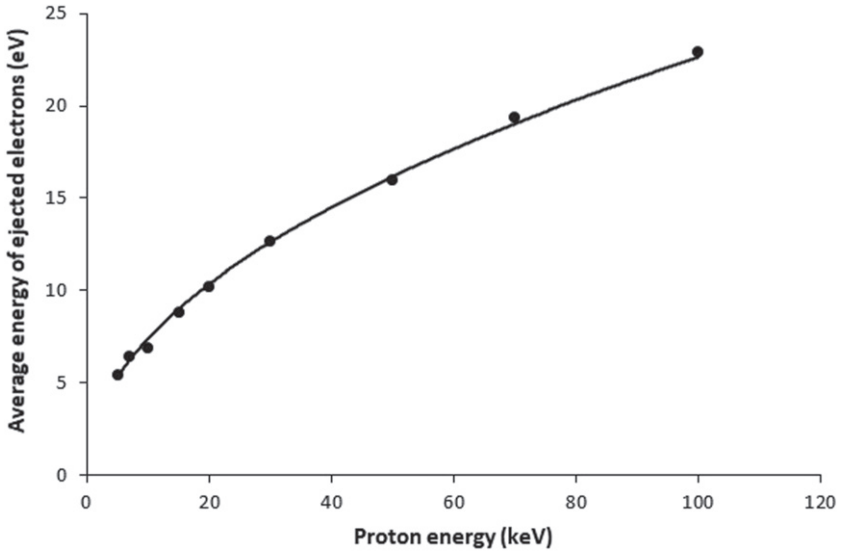

Figure 2. The average energy of ejected electrons in $H^+ + H_2$ collisions.

3. The basic space charge compensation model

3.1. Processes, cross-sections and rates

The basic process of space charge compensation involves the production of slow ions and electrons by the beam components. The electrons are trapped in the beam potential and reduce its magnitude and the slow ions are expelled from the beam due to the resulting potential.

The slow ions are produced in a number of ways. The ion beam will ionize the background gas. Charge exchange between the ion beam and the background gas will also produce slow ions. The cross-sections for these processes are σ_{i} and σ_{cx} respectively. Since the beam under consideration also contains neutral components these can also ionize the background gas with an associated cross-section $\sigma_{0\mathrm{i}}$.

Electrons to be used in the compensation of the beam potential are produced initially in the ionization of the background gas by the beam ions. Rudd [7] has measured both the energy and angular distribution of electrons produced in ion collisions with gases. For the case of H^+ collisions with H_2 the average energy of the ejected electrons integrated over all angles is plotted in figure 2 against the proton energy.

The data for this average energy, E_{r}, is empirically fitted by the equation

$$E_{\mathrm{r}} = 0.084\left(\frac{E_{\mathrm{b}}}{K}\right)^{0.4861}, \tag{1}$$

where E_{b} is the beam acceleration energy in eV and K is the ion mass number. Theoretically the exponent is 0.5. The mass dependence has been added to allow scaling to other species. Rudd also found that the differential cross-section with respect to energy i.e. the cross-section for ejection of electrons with a given energy versus the energy of the ejected electrons was almost exponential. Thus, the ejected electrons have a wide distribution of energies that is exponential in form.

Electrons will also be produced in the ionization of the background gas by the neutral components of the beam. It is assumed here that the average energy and the energy distribution are the same as those produced in ionization by the ion beam components.

Electrons are also produced in stripping or re-ionisation of the neutral components on the background gas with a cross-section $s_{0\mathrm{s}}$. In this case the electrons are initially monoenergetic with a velocity equal to the beam component velocity and their energy, E_{s}, is then

$$E_{\mathrm{s}} = \frac{m_{\mathrm{e}}E}{Km_{\mathrm{p}}}E_{\mathrm{s}} = \frac{m_{\mathrm{e}}E}{Km_{\mathrm{p}}}, \tag{2}$$

where m_{e} are m_{p} are the electron and proton masses respectively. E is the beam component energy. It is argued in the appendix that these electrons from the various processes form thermal distributions. These will have a characteristic temperature $T_{\mathrm{s}} = 2E_{\mathrm{s}}/3$. These electrons have high enough energies to contribute to the ionization of the background gas with rate $\langle\sigma v\rangle_{\mathrm{ie}}$.

The cross-sections and rate used are empirical fits to those from the IAEA Aladdin database [8] except for the cross-section for ionization of the gas by the beam ions. Rudd [7] has measured cross-sections for this process and these have been used to be consistent with the use of the average ejected electron energies. It is worth noting though that Rudd's cross-sections are significantly higher than the database values by ~50% in the proton energy range 20–100 keV. The electron ionization rate for deuterium is assumed to be the same as for hydrogen. The equilibrium fractions have been taken from the ORNL red book [9]. All cross-sections for hydrogen collisions have been scaled using a constant velocity to other isotopes such as deuterium. So

$$v_{\mathrm{b}} = \left(\frac{2eE_{\mathrm{b}}}{M_{\mathrm{b}}}\right)^{0.5} = \left(\frac{2eE_{\mathrm{b}}}{Km_{\mathrm{p}}}\right)^{0.5} = \left(2eE_{\mathrm{bH}}/m_{\mathrm{p}}\right)^{0.5},$$

where M_{b} is the beam ion mass and $E_{\mathrm{bH}} = E_{\mathrm{b}}/\mathrm{K}$ is the equivalent proton energy.

In the following analysis it is assumed that the beam profile is parabolic for both ions and neutrals. As the ultimate intention is to examine the beam optics in the presence of a beam plasma and its associated potentials, it is useful to have a definition of the beam radius. The distribution of beam ion density is characterized by a single radial parameter, the beam radius, A, which is defined by the outer limit where the density is zero. Other profiles could be considered, for example a Gaussian profile but that implies that the beam still has a significant density at a multiple of the beam radius with consequent beam scraping and more complex mathematical expressions. In a subsequent paper, the dependence of the beam radius, A with the space charge electric field will be explored. The notation is used that n_{bx} or n_{0x} is the ion beam or neutral density of energy component x, with x being 1, 2 or 3 representing the full, half or third energy component respectively. In a similar way the axial densities are designated n_{b0x} or n_{00x}. For the case of the ion beam components then the profile is

$$n_{bx}(r) = n_{b0x}\left(1 - r^2/A^2\right), \tag{3}$$

where r is the radial dimension and A is the beam half width. It might be argued that a Gaussian profile for the beam is more suitable in view of the discussion in reference [6]. However, as the beam travels inside a fairly close-fitting pipe (the neutraliser or bending magnet) for most of its axial flight path, the beam density must be zero at the outer limit indicated by the A term above. This does not mean that all parameters must have such a profile.

Using the fractions of the extracted ion components and the equilibrium fractions of the neutral beam, the axial ion densities can be found from

$$\frac{If_1(1-F_1)}{e} = 2\pi\int_0^A n_{b1}(r)\, v_{b1} r\mathrm{d}r = \frac{\pi A^2}{2} n_{b01} v_b, \tag{4}$$

where I is the extracted current, f_1 is the extracted fraction of full energy ions and $(1 - \mathrm{F_1})$ is the equilibrium fraction of full energy ions after the neutraliser, v_{b1} is the velocity of the full energy ion component which is just designated v_b. Thus the axial ion densities for the three components are

$$\begin{aligned} n_{b01} &= \frac{2If_1(1-F_1)}{\pi e A^2 v_b} \\ n_{b02} &= \frac{2^{1.5} x 2If_2(1-F_2)}{\pi e A^2 v_b} \\ n_{b03} &= \frac{3^{1.5} x 2If_3(1-F_3)}{\pi e A^2 v_b} \end{aligned}. \tag{5}$$

In equation (5) the factor 2 comes from the profile definition. The factors $2^{1.5}$ and $3^{1.5}$ appearing arise from two causes. For instance, for the half energy component there is a factor $2^{0.5}$ from the relation between v_{b2} and v_b and a factor 2 because the $D_2{}^+$ (E_b) will end up as two D^+ ($E_b/2$). The total axial beam density is then

$$n_{b0} = n_{b01} + n_{b02} + n_{b03}. \tag{6}$$

Similarly, density equations can be written for the neutral components e.g. the full energy component density is

$$n_{01} = \frac{2If_1F_1}{\pi e A^2 v_b}$$

and the total axial neutral density is

$$n_{00} = n_{001} + n_{002} + n_{003}. \tag{7}$$

The total production rate, Q_{bi} ($\mathrm{m^3\ s^{-1}}$) on axis of slow ions and fast ejected ('Rudd') electrons by the ion beam components can then be written down as:

$$Q_{bi} = Nv_b\left(n_{b01}\sigma_i(E_b) + \frac{n_{b02}\sigma_i\left(E_b/2\right)}{\sqrt{2}} + \frac{n_{b03}\sigma_i\left(E_b/3\right)}{\sqrt{3}}\right),$$

where N is the gas density. Eliminating the individual ion densities gives

$$\begin{aligned} Q_{bi} = \frac{2IN}{\pi e A^2}\big(&f_1(1-F_1)\sigma_i(E_b) \\ &+ 2f_2(1-F_2)\sigma_i\left(E_b/2\right) + 3f_3(1-F_3)\sigma_i\left(E_b/3\right)\big), \end{aligned} \tag{8}$$

An equivalent equation for the production rate of ions and fast Rudd electrons by the neutral species, Q_{0i}, can then also be derived

$$\begin{aligned} Q_{0i} = \frac{2IN}{\pi e A^2}\big(&f_1F_1\sigma_{0i}(E_b) + 2f_2F_2\sigma_{0i}\left(E_b/2\right) \\ &+ 3f_3F_3\sigma_{0i}\left(E_b/3\right)\big). \end{aligned} \tag{9}$$

The neutral components can also be re-ionised or stripped on the background gas to produce a fast beam ion and an electron with energy given by equation (2). The rate, Q_{0s}, for this process is then

$$\begin{aligned} Q_{0s} = \frac{2IN}{\pi e A^2}\big(&f_1F_1\sigma_{0s}(E_b) + 2f_2F_2\sigma_{0s}\left(E_b/2\right) \\ &+ 3f_3F_3\sigma_{0s}\left(E_b/3\right)\big). \end{aligned} \tag{10}$$

By similar arguments the production rate of slow ions by charge exchange, Q_{cx}, is

$$\begin{aligned} Q_{cx} = \frac{2IN}{\pi e A^2}\big(&f_1(1-F_1)\sigma_{cx}(E_b) + 2f_2(1-F_2)\sigma_{cx}\left(E_b/2\right) \\ &+ 3f_3(1-F_3)\sigma_{cx}\left(E_b/3\right)\big). \end{aligned} \tag{11}$$

Taking n_{r0} to be the axial density of Rudd electrons from ionization by the ion and neutral components and stripped electrons the axial production rate of slow ions and also the production rate of slow electrons by these electrons is then

$$Q_e = Nn_{r0}\langle\sigma v\rangle_{ie}. \tag{12}$$

Hence the total production rate of slow ions, Q_i, is the sum of the process rates above

$$Q_i = Q_{bi} + Q_{0i} + Q_{cx} + Q_e. \tag{13}$$

The mean fast electron temperature, T_r, is then

$$Q_r = Q_{bi} + Q_{0s}. \tag{14}$$

As can be seen there are fewer plasma electrons formed than slow positive ions. The Rudd/stripped electrons escape easily from the beam plasma and always are treated separately. Due to the energies of the ion and neutral beam components there are three temperatures of the Rudd electrons from ionization by both ions and neutrals, T_{rx} with $x = 1, 2, 3$ referring to the full, half and third energy ions and neutrals. In addition, there are three temperatures of stripped electrons T_{sx}. It is convenient to use a single weighted average value to replace these six values. This is justified in the appendix. The weighting is the relative electron production cross-sections. This weighted average value of the fast electron temperature can be written as

$$T_r = \frac{\left[\sum_{x=1}^{x=3} T_{rx} f_x x \left(1 - F_x\right) \sigma_{bi}\left(\frac{E_b}{x}\right) + \sum_{x=1}^{x=3} T_{rx} f_x x F_x \sigma_{0i}\left(\frac{E_b}{x}\right) + \sum_{x=1}^{x=3} T_{sx} f_x x F_x \sigma_{0s}\left(\frac{E_b}{x}\right)\right]}{\left[\sum_{x=1}^{x=3} f_x x \left(1 - F_x\right) \sigma_{bi}\left(\frac{E_b}{x}\right) + \sum_{x=1}^{x=3} f_x x F_x \sigma_{0i}\left(\frac{E_b}{x}\right) + \sum_{x=1}^{x=3} f_x x F_x \sigma_{0s}\left(\frac{E_b}{x}\right)\right]}. \tag{15}$$

Substitution of values shows that T_r is close to the temperature of most of the individual Rudd/stripped temperatures but smaller than that for the full energy stripped electrons. This average temperature can be used in the evaluation of the slow electron and slow ion production in equations (12) and (13).

In the following sections ion beam heating of the plasma through Coulomb interactions will be discussed. It is convenient now to define the parameter, S_b given by

$$S_b = K^{1/2} \sum_{x=1}^{3} \frac{n_{b0x}}{\left(E_b/x\right)^{0.5}}. \tag{16}$$

This is introduced to simplify a later equation.

3.2. Electron confinement

The model needs an empirical form of the beam space potential variation with radius to proceed further. The following empirical equation for the space potential is proposed:

$$\phi(r) = -V_0\left(1 - \exp\left(-\alpha r^2\right)\right), \tag{17}$$

where ϕ and V_0 are in units of eV. At low values of r near the beam axis, this gives $\phi = -\alpha V_0 r^2$ which the required form shown by Holmes [6] for the freefall case so that the near axis ionic velocity is proportional to radius when weighted for production rate. A fuller explanation is given in [6].

However, the drift motion of the plasma ions at high pressure must also be examined. In this instance the ionic drift velocity, v_i, is:

$$v_i = \frac{k_i E}{N}.$$

As both the ionic mobility, k_i, and gas density, N, are constants, and v_i must be proportional to radius to obtain a constant plasma density near the axis, then the electric field must be proportional to the radius or the potential is proportional to r^2 similar to the free fall case.

The values of V_0 and α determine the shape of the potential. The convention chosen is that V_0 and α are positive numbers such that the potential on the beam axis is zero and $-V_0$ at the outer wall. Note that part of V_0 can exist within a narrow sheath adjacent to the wall as will be seen later.

The fast electrons with temperature T_r are confined within this potential. Their production rate within a volumetric element of length L and radius equal to the beam radius, A, must equal their loss through the surface of the element due to their thermal flux.

These electrons can flow axially or radially. However, the plasma potential as seen below is relatively low and for axial flow the interaction length is large relative to the radius (at least 50 fold) so as the velocity will be of the drift type and scales as $E/N = \phi/LN$ which is obviously small relative to the radial velocity which scales as ϕ/AN. The plasma exhaust also scales as the external surface area so that it is expected that the axial loss is then proportional to $\pi A^2 \times \phi/LN$ relative to a total radial loss of $2\pi AL \times \phi/AN$. If A/L equals 1/50 then for equal potentials the axial flow is then only 1/500 of the radial plasma loss and can be safely ignored.

Thus:

$$L\int_0^A Q_r\left(1 - \frac{r^2}{A^2}\right) 2\pi r \mathrm{d}r = \frac{n_{r0} v_r}{4} 2\pi AL \exp\left(\phi/T_r\right),$$

where n_{r0} and v_r are the axial density and the velocity of the fast or Rudd electrons. These electrons are deemed to escape when they reach the outer wall at potential $-V_0$ and so

$$n_{r0} = \frac{AQ_r}{v_r} \exp\left(V_0/T_r\right). \tag{18}$$

This density scales as $(NI/A)\exp(V_0/T_r)$. The confinement of the thermal plasma electrons can be dealt with in an entirely analogous way leading to an equation for their axial density, n_{e0}, with temperature T_e and velocity v_e,

$$n_{e0} = \frac{AQ_e}{v_e} \exp\left(V_0/T_e\right). \tag{19}$$

It is assumed that the fast electrons have the same spatial distribution as the beam ions.

3.3. The energy balance

The plasma electrons have been considered, in earlier work [3, 4] to have been heated only by the beam ions through Coulomb interactions as discussed earlier. In this section, heating by the fast Rudd and stripped electrons is also taken into account. The heating of the plasma electrons by the ion beam

will be considered firstly for the case of the full energy beam. The total energy transfer rate from ions to the electrons, n_{be}, is given by the NRL plasma formulary [10]

$$\nu_{be} = 2\nu_s - \nu_{//} - \nu_{\perp}, \tag{20}$$

where ν_s, $\nu_{//}$ and $\nu_{\perp}$ are the rates for slowing, parallel and perpendicular energy transfer respectively. Using explicit expressions for these rates gives

$$\nu_{be} = n_{e0}\lambda\left(\frac{2K^{1/2}1.7\times10^{-10}}{E_b^{3/2}} - \frac{1.8\times10^{-13}}{K^{1/2}E_b^{3/2}} - \frac{K^{1/2}T_e 1.7\times10^{-10}}{E_b^{5/2}}\right), \tag{21}$$

where K is the mass number of the beam ions and λ is the Coulomb logarithm and this has a value of approximately 7. Note that [10] uses densities in units of cm^{-3} but equation (21) has densities in units of m^{-3}. The temperatures and energies and temperatures are in units of eV and are multiplied by e to give the energy in Joules. Inspection of the terms in equation (21) shows that the second term is much smaller than the first. The third term is also much smaller than the first if T_e is much less than the beam energy which is indeed the case. Thus

$$\nu_{be} = n_{e0}\lambda\left(\frac{2K^{1/2}1.7\times10^{-10}}{E_b^{3/2}}\right). \tag{22}$$

The actual energy transferred by a beam ion, E_i, is

$$E_i = 3.4\times10^{-10}\frac{K^{1/2}n_{e0}\lambda}{E_b^{3/2}}eE_b\tau_b, \tag{23}$$

where τ_b is the transit time of a beam ion through a volume of plasma. This is simply L/v_b with L being the length of the plasma volume and v_b the beam velocity. Hence rationalizing for each species x gives

$$E_{ix} = 3.4\times10^{-10}\frac{K^{1/2}x^{1/2}n_{e0}\lambda}{E_b^{1/2}}\frac{eL}{v_{bx}}. \tag{24}$$

In the case of heating of the plasma electrons by the fast Rudd and stripped electrons, the appropriate NRL equations [10] are used again. The slowing frequency, ν_s, is equal to the perpendicular frequency, $\nu_{\perp}$, and the parallel frequency, $\nu_{//}$, is lower than these by a factor $\sim 2T_r/T_e$. Hence the energy transfer rate (in SI units) from the fast electrons to the plasma electrons is

$$\nu_{re} = 7.7\times10^{-12}\frac{n_{e0}\lambda}{T_r^{3/2}}. \tag{25}$$

Thus, the total energy input, E_{re}, to the thermal electron distribution per fast electron (in Joules) during its confinement time, τ_r, is

$$E_{re} = 7.7\times10^{-12}\frac{n_{e0}\lambda}{T_r^{3/2}}eT_r\tau_r. \tag{26}$$

If the axial density of the beam component, n_{b0x}, is used to obtain production rates then the effective volume of the beam is then:

$$\text{volume} = \frac{L\int_0^A n_{box}\times\left(1-r^2/A^2\right)\times2\pi r\mathrm{d}r}{n_{b0x}} = \pi A^2L/2.$$

The next stage is to calculate how many new beam ions in the beam volume $\pi A^2L/2$ per second which is:

$$\frac{\pi A^2L}{2}\sum_{x=1}^{3}n_{b0x}v_{bx}.$$

The thermal electrons leave the plasma with their energy eT_e and assuming they are also bound by the potential V_0 the energy balance is then

$$3.4\times10^{-10}\frac{n_{e0}\lambda K^{\frac{1}{2}}}{E_b^{\frac{1}{2}}}\sum_{x=1}^{3}x^{\frac{1}{2}}n_{b0x}\frac{eL\pi A^2}{2} + 7.7\times10^{-12}\frac{n_{e0}\lambda}{T_r^{\frac{3}{2}}}eT_r\tau_r\frac{Q_r\pi A^2L}{2} = \frac{n_{e0}v_e eT_e}{4}2\pi AL\,\exp\left(-V_0/T_e\right)$$

or

$$3.4\times10^{-10}\lambda AK^{1/2}\sum_{x=1}^{3}\frac{x^{1/2}n_{b0x}}{E_b^{1/2}} + 7.7\times10^{-12}\frac{\lambda}{T_r^{3/2}}T_r\tau_rQ_rA = v_eT_e\,\exp\left(-V_0/T_e\right).$$

Each fast electron once created transfers an energy E_r to the thermal population so the total energy transfer depends on the total rate of ionization. The volumetric production rate is equal to the density of fast electrons divided by the confinement time i.e. $Q_r = n_{r0}/\tau_r$ giving

$$\lambda A\left(3.4\times10^{-10}K^{1/2}\sum_{x=1}^{3}\frac{x^{1/2}n_{b0x}}{E_b^{1/2}} + 7.7\times10^{-12}\frac{n_{r0}}{T_r^{1/2}}\right) = v_eT_e\,\exp\left(-V_0/T_e\right)$$

or

$$\lambda A\left(3.4\times10^{-10}S_b + 7.7\times10^{-12}\frac{n_{r0}}{T_r^{1/2}}\right) = v_eT_e\,\exp\left(-V_0/T_e\right), \tag{27}$$

where the parameter S_b has been used from equation (16). This gives the energy balance in the plasma where Coulombic heating of the plasma electrons by the beam and fast electrons is balanced by the energy lost as they escape from the potential.

4. The drift and freefall approximations

Consideration is now given to the two approximations of how the secondary slow ions move out of the beam under the influence of the beam potential; namely the drift and freefall approximations. These two methods of deriving the ion velocity exist in all plasma modelling with the former applying when the plasma dimension is larger than the ion-neutral mean free path. For example, in plasma sheaths, whose width is a few Debye lengths, the ion motion is free fall whereas in the main body of the plasma the motion is normally collisional drift and

so both exist at the same time. As the beam can operate at low and high pressures any model must encompass both modes of plasma ion motion. In the drift approximation the ions are collisional and freefall only exists in the presheath at the beam edge. In the freefall approximation the ions move solely under the influence of the potential between the point where they are created and that towards the edge of the beam. They are in freefall throughout the entire beam. In the presheath for the drift situation, whose width is roughly the Debye length, it is somewhat similar as the plasma ions are considered collisionless and hence move by free-fall. In the free fall case, there is no presheath and the freefall region extends from the beam centre to the outer edge. The applicability of these approximations is discussed later.

4.1. The drift approximation

From Kaye and Laby [11] the drift velocity, v_i, of hydrogen ions in their parent gas under the influence of an electric field of 1 V m^{-1} is 1.13×10^{-4} ms^{-1} for a gas density of $N = 2.68 \times 10^{25}$ m^{-3} at 273 K. This drift velocity is related to the general mobility k_i by, as stated earlier,

$$v_\mathrm{i} = \frac{k_\mathrm{i} E}{N}.$$

This gives a value for k_i of 3.03×10^{22} m^5 s^{-1} V^{-1}. For deuterium a factor of $1/\sqrt{2}$ has to be applied. The electric field can be found from the potential ϕ in equation (17) to give

$$v_\mathrm{i} = \frac{k_\mathrm{i} E}{N} = \frac{k_\mathrm{i}}{N} 2 V_0 \alpha r \exp\left(-\alpha r^2\right). \tag{28}$$

Then in any annular ring at radius r the local ion density is given by

$$2\pi r n_\mathrm{i} v_\mathrm{i} = Q_\mathrm{i} \pi r^2 \left(1 - \frac{r^2}{2A^2}\right),$$

where Q_i is the total slow ion production rate given in equation (13). Hence the ion density, n_i, is

$$n_\mathrm{i} = \frac{Q_\mathrm{i} \frac{rN}{2} \left(1 - \frac{r^2}{2A^2}\right)}{k_\mathrm{i} 2 r \alpha V_0 \exp\left(-\alpha r^2\right)}.$$

At low values of r the axial slow ion density, n_i0, is then

$$n_\mathrm{i0} = \frac{QN}{4 k_\mathrm{i} \alpha V_0}. \tag{29}$$

At this stage plasma neutrality is invoked

$$n_\mathrm{i0} = n_\mathrm{e0} + n_\mathrm{r0} - n_\mathrm{b0}. \tag{30}$$

Experimentally it is known that the total potential across the beam must be very low otherwise the beam would 'blow up' through space charge repulsion. Below an estimate of the total potential of the un-neutralised beam corresponding to the JET beam is of the order of 158 kV, which would cause the beam to diverge to 90 degrees within one beam diameter ($2A$) along the beam axis. This clearly does not happen so the potential across the beam must be small compared to the above value. All beams everywhere are similar in this respect and reference [6] discusses this in more detail. This means that space charge neutrality as shown in equation (30) must be satisfied to a very high degree and the equality can be applied for this theoretical model. A justification for the use of plasma neutrality and an estimation for the degree of plasma neutrality is given later.

If V_0 and T_e are known, the two electron and the beam densities can be determined and this gives a method of determining the product αV_0

$$[\alpha V_0]_a = \frac{QN}{4 k_\mathrm{i} n_\mathrm{i0}}. \tag{31}$$

The subscript 'a' refers to the first method of determining this product.

A balance for the slow ions can also be established for the whole beam where the ion production is balanced by the ions leaving the beam at the ionic sound speed, c_s. This gives

$$L \int_0^A Q_\mathrm{i} 2\pi r \mathrm{d}r = L Q_\mathrm{i} \frac{\pi A^2}{2} = n_\mathrm{i0} 2\pi A L c_\mathrm{s},$$

where the ionic sound speed (or Bohm velocity) is

$$c_\mathrm{s} = 0.6 \left(\frac{e T_\mathrm{e}}{M_\mathrm{i}}\right)^{0.5}$$

with M_i being the plasma ion mass. The factor of 0.6 accounts for the density drop across the presheath. Substituting for n_i0 gives the second method ('b') of determining the product αV_0.

$$[\alpha V_0]_\mathrm{b} = \frac{0.6N}{k_\mathrm{i} A} \left(\frac{e T_\mathrm{e}}{M_\mathrm{i}}\right)^{0.5}. \tag{32}$$

In order to solve the drift equations an initial value of V_0 is provided which allows the fast electron density n_r0 to be calculated. Using equation (27) a value of the plasma electron temperature, T_e, can be determined. This equation is transcendental but can be solved by iterative methods such as Newton–Raphson. With knowledge of T_r, T_e and n_r0 and n_e0 can be calculated using equation (19) leading to values of $[\alpha V_0]_a$ and $[\alpha V_0]_b$ from equations (31) and (32). These values will not generally be equal for an arbitrary guess for V_0 and the difference between them can be used to update the value of V_0. This process is repeated until a satisfactory convergence criterion has been satisfied. Note that V_0 is being iterated to give closely equal values of $[\alpha V_0]_a$ and $[\alpha V_0]_b$ and these have the same dependence on the ion mobility k_i, V_0 is independent of k_i but not α.

4.2. The freefall approximation

In the drift case, the plasma ion velocity is a locally determined parameter set by the local value of the electric field divided by the gas density and multiplied by the mobility constant. In the free fall situation however, the velocity at some radius, r, is not set locally but also depends where that plasma ion was created at some smaller radius, a, so that

$$v(r) = \left(\frac{2e}{M_\mathrm{i}}\right)^{0.5} (\phi(a) - \phi(r))^{0.5}.$$

In this approximation the ions move under the influence of the potential from where they are created until they escape the beam. Thus, the slow ion balance becomes after integrating over all possible creation radius values:

$$2\pi r n_{\mathrm{i}}(r) = Q_{\mathrm{i}} \int_0^r \frac{2\pi a \mathrm{d}a}{\left(\frac{2e}{M_{\mathrm{i}}}\right)^{0.5} \left(\phi(a) - \phi(r)\right)^{0.5}}. \tag{33}$$

Note that the value of Q_{i} is treated as a constant although strictly it too would have a radial dependence. This purely for mathematical convenience and a more sophisticated treatment could remove this limitation. The potential (17) can be expanded as

$$\phi(r) = -V_0 \alpha r^2 + \frac{V_0 \alpha^2 r^4}{2}.$$

The integral is only finite if the first term is quadratic [6] which gives

$$n_{\mathrm{i}}(r) = \frac{Q}{r\left(\frac{2e}{M_{\mathrm{i}}}\right)^{0.5}} \int_0^r \frac{a \mathrm{d}a}{\left(V_0 \alpha r^2 - V_0 \alpha a^2\right)^{0.5}}.$$

Or limiting this expression to the axial value this becomes

$$n_{\mathrm{i0}} = \frac{Q_{\mathrm{i}}}{\left(\frac{2e\alpha V_0}{M_{\mathrm{i}}}\right)^{0.5}}. \tag{34}$$

Using plasma neutrality as in the drift case, n_{i0} can be calculated and then equation (34) allows a value of αV_0 to be determined. In this case V_0 and α cannot be separated.

Again, applying the ion balance equation

$$2\pi A L n_{\mathrm{i0}} v_{\mathrm{i}} = 2\pi L \int_0^A Q_{\mathrm{i}} \left(1 - \frac{r^2}{A^2}\right) r \mathrm{d}r, \tag{35}$$

where v_{i} is now not the ion sound speed but the average velocity acquired by the ions and is defined as

$$v_{\mathrm{i}} = \left(\frac{2e\langle U_{\mathrm{i}}\rangle}{M_{\mathrm{i}}}\right)^{0.5} \tag{36}$$

with $\langle U_{\mathrm{i}}\rangle$ being the average energy gained by the ions whilst in the beam. This energy is $V_0 + \phi(r)$ and so the average value $\langle U_{\mathrm{i}}\rangle^{0.5}$ is

$$\langle U_{\mathrm{i}}\rangle^{0.5} = \frac{\int_0^A 2\pi r Q_{\mathrm{i}} \left(1 - \frac{r^2}{A^2}\right) \left(V_0 + \phi(r)\right)^{0.5} \mathrm{d}r}{\int_0^A 2\pi r Q_{\mathrm{i}} \left(1 - \frac{r^2}{A^2}\right) \mathrm{d}r}..$$

Or, on using the potential from equation (17) this becomes

$$\langle U_{\mathrm{i}}\rangle^{0.5} = \frac{2V_0^{0.5} \int_0^A \left(1 - \frac{r^2}{A^2}\right) \exp\left(-\frac{\alpha r^2}{2}\right) r \mathrm{d}r}{2\int_0^A r \left(1 - \frac{r^2}{A^2}\right) \mathrm{d}r}.$$

This is integrated to give

$$\langle U_{\mathrm{i}}\rangle^{0.5} = \frac{V_0^{0.5}\left[2\exp\left(-\frac{\alpha A^2}{2}\right) + \alpha A^2 - 2\right]}{\frac{\alpha^2 A^4}{4}}.$$

Setting $W = \alpha A^2/2$ this is

$$\langle U_{\mathrm{i}}\rangle^{0.5} = \frac{2V_0^{0.5}}{W^2} \times \left[\exp(-W) + W - 1\right]. \tag{37}$$

Substituting for n_{i0}, v_{i}, and $\langle U_{\mathrm{i}}\rangle$ from equations (34), (35) and (37) into the slow ion balance equation (34) then leads to

$$\frac{(2W)^{0.5} W^2}{8} = \left[\exp(-W) + W - 1\right]. \tag{38}$$

This has the unique solution

$$W = \frac{\alpha A^2}{2} = 2.271\,44. \tag{39}$$

Or

$$\alpha = \frac{4.542\,88}{A^2}. \tag{40}$$

This determines a for any value of beam radius and is independent of gas density unlike the drift model. Since α is known V_0 can be determined from the product αV_0 found from equation (34).

The solution to the freefall equations initially follows that for the drift equations. From an initial value of V_0 the fast electron density n_{r0} can be calculated. Using equation (27) a value of the plasma electron temperature, T_{e}, can be determined. This then allows n_{e0} can be calculated using equation (19). From plasma neutrality, the slow ion density n_{i0} is then calculated and since α is known from the chosen beam radius through equation (40) a new value of V_0 is determined from equation (34). From the initial guess of V_0 and its updated value a new estimate is made and the procedure is repeated until the value of V_0 has converged to a suitable degree.

5. Results and discussion

5.1. General results

In order to illustrate the power of the model it has been applied to the nominal 120 kV, 60 A beam referred to earlier. For this beam the flux fractions of the D^+, $D_2{}^+$ and $D_3{}^+$ ions, f_1:f_2:f_3 are ~0.72:0.22:0.06. In figure 3 the potential, V_0, and plasma electron temperature, T_{e}, are plotted against the background gas pressure for a beam of nominal radius $A = 0.1$ m.

At low pressures the models both show potentials and plasma temperatures which are close to each other of approximately 90 eV and 12 eV respectively. As the pressure increases the potential and electron temperature fall. The electron temperature falls as the gas density increases due to increased collisionality and since the potential can be related to the electron temperature this falls also. At the highest densities heating of the plasma has more of an effect in the drift approximation. The predictions of the two models separate with the drift model giving a higher potential and plasma temperature than the freefall model. At the highest pressure shown of 3 $\times$ 10^{20} m^{-3} the potential is ~40 eV for the drift model and approximately half that for the freefall.

The axial densities of the plasma electrons ($n_{\mathrm{e0}}/n_{\mathrm{b0}}$), slow positive ions ($n_{\mathrm{i0}}/n_{\mathrm{b0}}$) and the fast electrons ($n_{\mathrm{r0}}/n_{\mathrm{b0}}$) relative to the beam ion density (n_{b0}) are shown in figure 4 for the two approximations.

The plasma electron and ion densities rise with increasing background gas pressure. In the freefall approximation the ion density is lower than the plasma electron density at

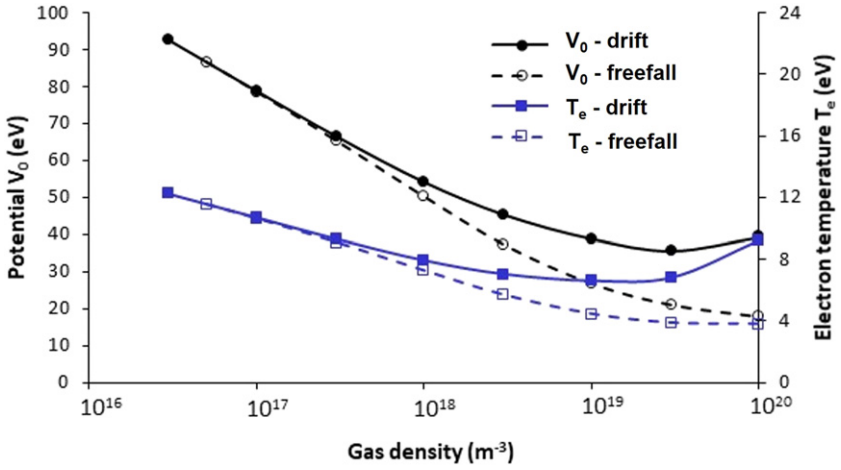

Figure 3. The potential V_0 and the plasma electron temperature T_e for a nominal 120 kV, 60 A deuterium beam with radius $A = 0.1$ m as a function of the background gas pressure in both the drift and freefall approximations.

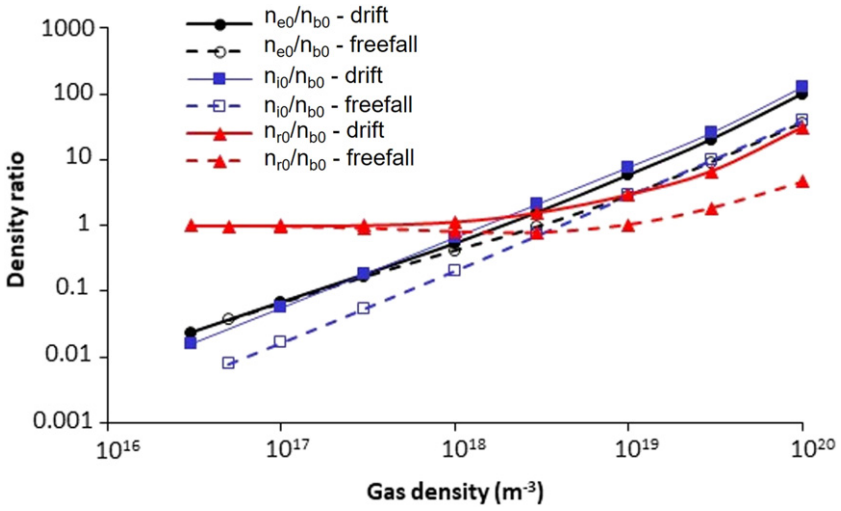

Figure 4. The axial densities of the plasma electrons (n_{e0}/n_{b0}), slow positive ions (n_{i0}/n_{b0}) and the fast electrons (n_{r0}/n_{b0}) relative to the beam ion density (n_{b0}) for the nominal 120 kV, 60 A beam with radius $A = 0.1$ m.

lower gas densities although they become equal at the higher gas densities. In the drift approximation the plasma electron and ion densities are almost equal at all gas densities. The fast electron density in the drift model increases slowly as the pressure increases since there is relatively little production of these electrons before their density increases more rapidly as the pressure increases. The density of these electrons is a balance between their production rate and the rate at which they escape from the beam due to their energy, the potential trying to retain them and the electron temperature. In the freefall model the fast electron density falls slightly as the pressure starts to increase. This is due to the ions being able to escape more easily and to maintain plasma neutrality the electron density reduces.

In figure 5 the ratio of the contributions of the beam and fast electron heating of the plasma is plotted for the two models. Over the whole range of the gas densities the electron heating of the plasma dominates that due to the beam itself. At low pressures both models give the beam to fast electron heating ratio as ∼0.7. At higher densities the freefall model indicates that these two contributions become almost equal but in both models this ratio falls with increasing density. At the highest gas density, the beam heating contribution becomes relatively small for both the drift and freefall models. This dominant electron heating of the beam plasma electrons was not considered by earlier workers [3–5].

The dependence of the potential and electron temperature on beam radius is shown in figure 6 for a background gas density of 3×10^{17} m^{-3}. Both the potential and the electron temperature decrease as the beam radius increases as the electrons remain within the beam due to its increased size. At this low gas density, the two models are in good agreement in accordance with figure 3.

As discussed earlier the ionization cross-sections from Rudd [7] have been used in the implementation of the model. These cross-sections are somewhat higher than those from the Aladdin database [8]. Using these latter cross-sections has only a small effect of a few percent on the potential V_0 and temperature T_e and the relative densities. The heating ratio is increased by up to ∼10% at intermediate gas densities.

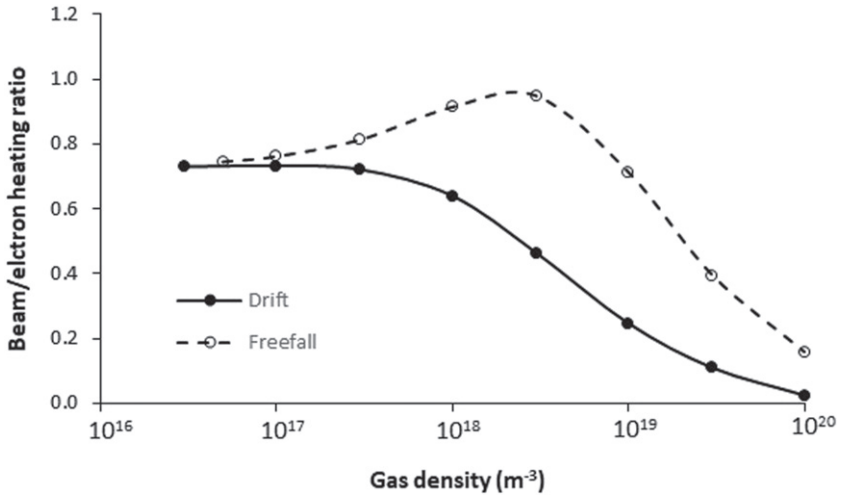

Figure 5. The ratio of the beam and fast electron heating contributions to the plasma electrons for the nominal 120 kV, 60 A beam with radius $A = 0.1$ m for the two models.

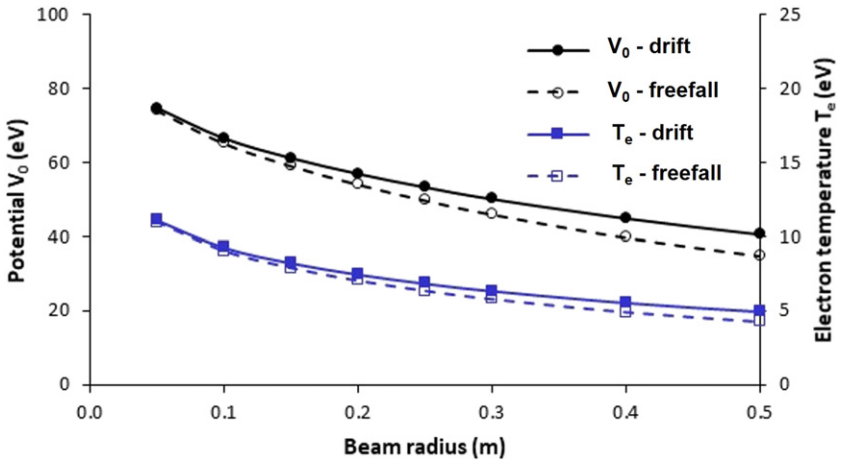

Figure 6. The dependence of the potential V_0 and the electron temperature T_e on beam radius for the nominal 120 kV, 60 A beam with a background gas density of 3×10^{17} m^{-3} for the two models.

Use of these cross-sections does not change the conclusions reached.

5.2. The potential and radial field

A plot of the radial potential is shown for the drift model in figure 7 at different gas densities and a beam radius $A = 0.1$ m. The potential is plotted against the radial distance r. At low gas densities there is very little potential drop between the axis and the beam radius although this does increase with gas density. Most of the potential drop is beyond the beam edge.

Although the drift and freefall models give similar results of V_0 and T_e at low gas densities the potential distributions are very different as shown in figure 8 for a gas density of 10^{17} m^{-3} and a beam radius of 0.1 m. In the case of the freefall model the value of the parameter α which defines the potential extent (equation (17)) is constant at all gas densities and from equation (40) it has in this case a value of ∼454 indicating that the potential drop is mostly within the beam as illustrated by figure 8.

Although the total potentials are similar at low pressure between freefall and drift, the fact that most of the potential drop occurs in an outer sheath beyond the beam edge for the drift case means that the electric field inside the beam which ultimately controls the beam divergence is much larger in the freefall case. In the freefall approximation the average electric field across the beam is, from figure 8, ∼700 V m^{-1} whereas it is almost zero for the drift approximation.

Earlier, plasma neutrality was assumed. Poisson's equation $E/A \sim e\Delta n/\varepsilon_0$ can be used to estimate the difference in positive and negative charge densities, Δn, that can establish this electric field E. Using 700 V m^{-1} and a beam radius of 0.1 m then $\Delta n \sim 4 \times 10^{11}$ m^{-3}. For this case the total electron (or positive ion density) is 4.73×10^{15} m^{-3}. Hence the fractional density difference is $\sim 8 \times 10^{-5}$ showing that plasma neutrality is indeed a reasonable assumption.

Measurements of the plasma produced by an ion beam have been made on low power beams previously; see [5, 6, 13] for example. However, Crowley *et al* [14] have succeeded in making measurements of the electron temperature, potential and electron density in the beam produced plasma of a JET Neutral

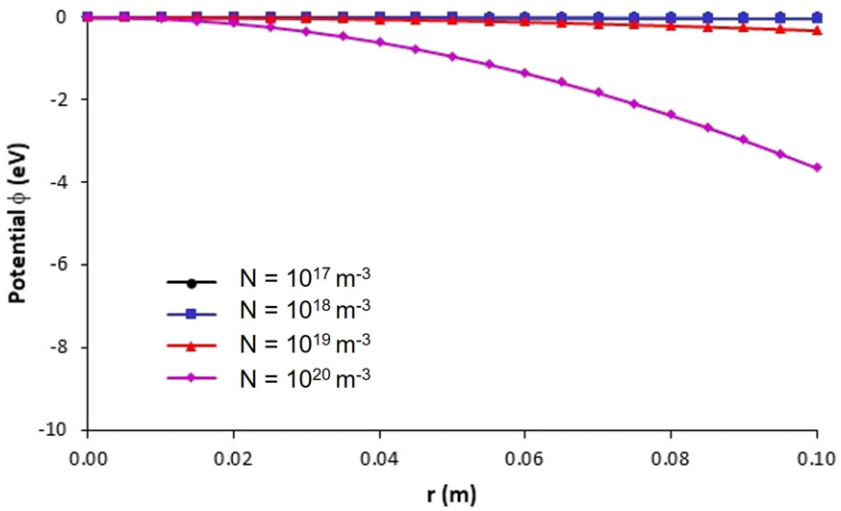

Figure 7. The radial potential dependence within the beam for a 120 kV, 60 A beam at different background gas densities for the drift model with a beam radius $A = 0.1$ m.

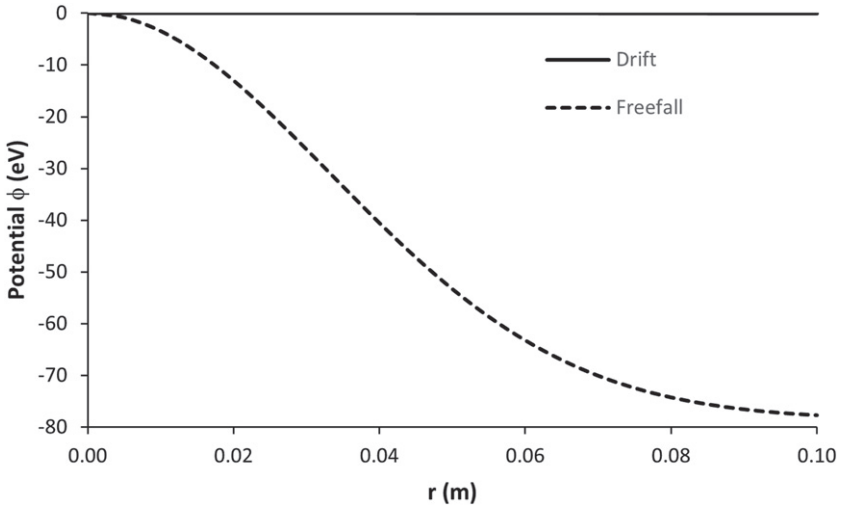

Figure 8. The radial potential dependences within the beam for a 120 kV, 60 A beam at a background gas density of 10^{17} m^{-3} with a beam radius $A = 0.1$ m for both the drift and freefall models.

Beam injector on the JET Neutral Beam Test Bed. Their measurements were made in the beam generated plasma in the gas neutralizer at about 1 m from the end of the neutralizer. At this position, the fractions of ions and neutrals are far from their equilibrium values. Hence a comparison between the model developed here and the results of those measurements cannot made since the model assumes the beam fractions are at their equilibrium values. An inferred method to compare the model with measurements is to look at the consequences of this potential such as on the beam optics. In the Neutral Beam Test Bed [12] the composite beam drifts for a distance of ~10 m in a vacuum chamber a low pressure. Any effect on the beam profile due to space charge effects might become apparent over this distance. Using the drift and freefall models the effect of the profile can be calculated and compared to measurements which may allow differentiation between the applicability of the models. This will be the subject of a future paper.

5.3. The applicability of the drift and freefall approximations

The question naturally arises as to the region of applicability of both approximations. The transition between the two approximations is taken to occur when the value of $1/N\sigma_s A \sim 1$ where σ_s is the scattering cross-section for slow ions leaving the beam. The theoretical value of the ion mobility is given by

$$k_i = \frac{e}{\sigma_s M_i c_T}, \tag{41}$$

where c_T is the thermal ion velocity. For deuterium $k_i = 2.1 \times 10^{22}$ m^5 s^{-1} V^{-1} and $c_T = 1250$ ms^{-1} giving a scattering cross-section of $\sigma_s = 9 \times 10^{-19}$ m^{-2}. Thus using this the transition between the approximations might be expected to occur at a product of gas density and radius of NA $\sim 1.1 \times 10^{18}$ m^{-2}. In the case of the example with $A = 0.1$ m the transition between the two models will be at a gas density of $\sim 1.1 \times 10^{19}$ m^{-3} (0.046 Pa or 4.5×10^{-4} mbar). From figure 3

the two approximations begin to diverge at a gas density of $\sim 5 \times 10^{17}$ m^{-3} which is somewhat lower than this simple estimate.

Although the drift approximation is more likely to apply at higher gas densities and given the situation shown in figure 8 where both approximations give similar V_0 and T_e but different potentials it would require measurement of the beam potential and plasma properties to distinguish between the two approximations.

For the JET neutral beam injectors, the gas target in the neutraliser is approximately 5×10^{19} m^{-2} which for the 2 m long neutraliser gives an estimate of the average gas density of 2.5×10^{19} m^{-3}. The model described here is only applicable downstream of the neutraliser when the species fractions are assumed to have reached their equilibrium fractions. Outside the neutraliser, the gas density is expected to fall very rapidly due to the very high pumping speed of approximately 10^6 s^{-1}. Typically the pressure in the injector vacuum system is less than 10^{-5} mbar (10^{-3} Pa or 2.4×10^{17} m^{-3}). This value of gas density is just within the region where both approximations give very similar results at least in terms of V_0 and T_e but as pointed out above there are important differences in the models.

5.4. The degree of space charge compensation

In designing neutral beam injection systems, it is generally assumed that there are no space charge forces involved. This makes it relatively straightforward to calculate the trajectories of the beam ions for instance as they move to residual ion dumps since the ions move independently of each other. If substantial potentials exist with the beam then space charge forces would need to be taken into account. In order to understand if this is the case the potentials can be compared with those of an uncompensated beam to give the degree of space charge compensation. The potential due to the beam when it is uncompensated can be calculated using Gauss's law.

$$\frac{Q}{\varepsilon_0} = \frac{e}{\varepsilon_0}\int n \mathrm{d}V = \int \boldsymbol{E}\cdot \mathrm{d}\boldsymbol{s}, \tag{42}$$

where Q is the total charge within some volume V, n is the charge density, E is the electric field and ds is an element of the surface enclosing the volume. Applying this to a cylindrical beam of length L gives an equation for the radial electric field component E_r

$$\frac{Q}{\varepsilon_0} = \frac{2\pi e L}{\varepsilon_0}\int_0^r r^{'} n_b\left(r^{'}\right)\mathrm{d}r^{'} = 2\pi r E_r L. \tag{43}$$

The beam density profile is given from equations (3), (5) and (6). Evaluation of the integral gives the radial electric field

$$\begin{aligned} E_r &= \frac{e n_{b0}}{\varepsilon_0}\left(\frac{1}{2}r - \frac{r^3}{4A^2}\right) \quad r \leqslant A \\ E_r &= \frac{e n_{b0}}{4\varepsilon_0 r}A^2 \quad r > A \end{aligned} \tag{44}$$

To obtain the potential distribution this equation can be integrated again using the condition that $V(r = 0) = 0$ to give

$$\begin{aligned} V(r) &= -\frac{e n_{b0}}{4\varepsilon_0}\left(r^2 - \frac{r^4}{4A^2}\right) \quad r \leqslant A \\ V(r) &= -\frac{e n_{b0} A^2}{4\varepsilon_0}\left(\frac{3}{4} - \ln\left(\frac{A}{r}\right)\right) \quad r > A \end{aligned} \tag{45}$$

The degree of space charge compensation, η, is defined as

$$\eta = 1 - \frac{\Delta\phi_c}{\Delta\phi_u}, \tag{46}$$

where $\Delta\phi_c$ and $\Delta\phi_u$ are the compensated and uncompensated potential differences across the beam. Strictly, the degree of space charge compensation is a local parameter. The definition in equation (46) is a useful average over the whole beam since the charge distributions have been integrated to give the electric field distribution and the potential difference across the beam. Using the data from figure 7, $\Delta\phi_c$ is 0.32 V for the drift approximation and 77.5 V for the freefall approximation. From equation (44) the uncompensated potential difference across the beam, $\Delta\phi_u$, is 158 kV. This indicates that in both approximations the beam is very highly compensated indeed. Incidentally, for a Gaussian beam distribution, an analytical expression for the electric field can be obtained [15] which contains a $1/r$ term as so the integral to obtain the potential diverges and the uncompensated potential cannot be obtained readily.

This beam consisting of a mixture of ions and atoms travels a distance of up to 2 m between the exit of the neutraliser and bend magnet where the ions are swept out of the beam unto beam dumps. At this stage the ions are separated and there is no longer a single beam. Up until that point space charge forces seem unlikely to have a noticeable effect on the beam transport. The magnet could affect the space charge neutralisation as both the fast electrons and plasma electrons are trapped by the magnetic field however there is no evidence of the separated ion species stalling under the influence of their own space charge. Before being installed on JET, the injectors are tested and characterized on the Neutral Beam Test Bed [12]. The composite beam travels a distance of 10 m on this facility. Although there are no obvious signs of space charge effects since the injector works on JET as expected a more detailed survey is to be carried out.

6. Conclusions

A model has been developed describing the process of space charge neutralisation in a beam consisting of a mixture of ion and atoms with different energies as used in the heating beams for fusion applications. The model is powerful in that it allows the beam potential and the plasma density and temperature to be calculated in both a drift and free fall approximation. When applied to a typical beam of 120 kV, 60 A the model shows that the beam is very highly compensated and so space charge forces play little or no role in the beam transport at least until the bend magnet is reached. There are outstanding questions such as which approximation is valid at low pressures and this will be studied in a subsequent paper.

It would be interesting to compare this model with numerical simulations of space charge compensation using codes such as SolMaxP [15, 17] and WARP [18] to understand the range of validity of the analytical model. Chauvin [17] has used the code to simulate transport of a 140 keV D^+ beam and this would be a useful study to compare the present model to.

The model can be easily adapted for use in a single species ion beam by choosing the beam parameters appropriately. It could also be modified to describe the space charge compensation in negative ion based beams such as those to be use in higher energy neutral beam injection for fusion applications.

Acknowledgments

This work has been carried out within the framework of the Contract for the Operation of the JET Facilities and has received funding from the European Union's Horizon 2020 research and innovation programme. The views and opinions expressed herein do not necessarily reflect those of the European Commission.

Appendix. Thermalisation of the fast electrons

In section 3.1, it was argued that the fast electrons should have an energy of 2/3 of the Rudd energy given in equation (1). This also applies to the stripped electrons. In this appendix this argument is examined. In order for these electrons to thermalize, they must undergo significant scattering before escape from the beam. There are two possible scattering events, scattering by gas collisions and/or via coulomb collisions. The *total* scattering cross-section via gas collisions, σ_s, is given in the database of Smith and Glasser [19] and has a value for electron collisions with H_2 of 1.4×10^{-19} m^2 for a Rudd energy of about 15 eV. These electrons will have a quasi-thermal distribution if the collision time is shorter than their confinement time in the beam. The collision frequency derived from coulomb scattering via the plasma ions and beam ions is smaller by a factor of about 20, even at low pressures and so will be ignored.

These fast Rudd electrons predominantly slow down via *inelastic* gas collisions such as excitation or ro-vibrational collisions. These collisions lead to a randomizing of the momentum vector of the colliding electrons and a loss of energy. There are very many such processes at low electron energies so it is expected that Coulomb thermalization which has a frequency of $8.2 \times 10^{-13} n \lambda T_r^{-1.5}$ will not dominate.

In view of the very many inelastic processes involved, the fast electrons are treated as a single fluid with a single temperature, T_r even though initially at least there will be three temperatures corresponding to the three beam energies from ionisation by ions and neutrals together with stripped electrons. During the slowing/energy loss process these individual populations will merge because the total electron–gas collision cross-section is moderately independent of electron energy at low energy [19], so faster electrons will have a higher collision rate than slower ones (via their higher velocity). This justifies a weighted average to derive a mean electron temperature.

It might be argued that the fast Rudd electrons should thermalize on the slow electrons but those slow electrons are in fact energy degraded Rudd electrons, produced somewhat earlier. The Coulomb interaction time is far too long for this to happen and instead the electron energy is expended in excitation and ro-vibrational collision.

As the collision processes randomize both the energy and momentum vector of electrons in a chaotic way, it is plausible in the absence of other information to argue that that this would lead to thermal distribution. It may not be truly Maxwellian but is more plausible than any other distribution and allows straightforward derivation of the plasma potential (equations (18) and (19)).

The gas collision frequency is $N\sigma_s v_r$ while the confinement time, τ_r, can be obtained from the expression:

$$L\int_0^A Q_r\left(1-\frac{r^2}{A^2}\right)2\pi r\mathrm{d}r \cong \frac{\pi L A^2 n_{r0}}{2\tau_r}.$$

This lhs of this expression was used in deriving equation (18) above. This leads to:

$$\tau_r = \frac{n_{r0}}{Q_r}.$$

Thermalization will occur if the product of the gas collision frequency and confinement time is at least unity. So:

$$\frac{n_{r0}}{Q_r} \times N\sigma_s v_r > 1.$$

As Q_r is proportional to Nn_{b0}, this ratio is independent of gas density. At low pressures, the ratio above is a little above unity indicating that a moderate amount of thermalization occurs. However, as n_{r0} becomes larger than n_{bo} at higher pressures as seen in figure 4 this ratio will become significantly greater than unity.

References

[1] Holmes A.J.T. 1987 *CERN Accelerator School* (Aarhus, Denmark) (http://dx.doi.org/10.5170/CERN-1987-010)
[2] Ćirić D. *et al* 2011 *Fusion Eng. Des.* **86** 509–12
[3] Gabovich M.D. 1977 *Sov. Phys. - Usp.* **20** 134
[4] Soloshenko I.A. 1998 *Rev. Sci. Instrum.* **67** 1346–52
[5] Winklehner D., Leitner D., Cole D., Machicoane G. and Tobos L. 2014 *Rev. Sci. Instrum.* **85** 02A739
[6] Holmes A.J.T. 1979 *Phys. Rev.* A **19** 389–407
[7] Rudd M.E. 1979 *Phys. Rev.* A **20** 787–96
[8] IAEA AMDIS Aladdin database (https://amdis.iaea.org/ALADDIN)
[9] Barnett C.F. *et al* 1977 *Atomic Data for Controlled Fusion Research ORNL-5206* (Oak Ridge National Laboratory)
[10] Richardson A. S. (NRL Plasma Formulary) 2019 (https://nrl.navy.mil/News-Media/Publications/NRL-Plasma-Formulary/)
[11] Kaye G.W.C and Laby T.H. Tables of chemical and physical constants (archived version at https://npl.co.uk/resources)
[12] McAdams R. *et al* 2015 *Fusion Eng. Des.* **96–97** 527–31
[13] Sherman J., Pitcher E. and Allison P. 1988 *Proc. 1988 Linear Accelerator Conf., CEBAF-R-89-001* (Williamsburg, VA)
[14] Crowley B., Surrey E., Cox S.J., Ciric D. and Ellingboe A.R. 2003 *Fusion Eng. Des.* **66–68** 591–6
[15] Chancé A., Chauvin N. and Duperrier R. 2012 *Proc. Int. Particle Accelerator Conf.* (New Orleans, USA)

[16] Chauvin N. 2012 *CERN Accelerator School* (Senec, Slovakia) (http://dx.doi.org/10.5170/CERN-2013-007)
[17] Chauvin N., Delferrière O., Duperrier R., Gobin R., Nghiem P.A.P. and Uriot D. 2012 *Rev. Sci. Instrum.* **83** 02B320
[18] Grote D.P. and Freidman A. 2005 *AIP Conf. Proc.* **749** 55
[19] Smith K. and Glasser A.H. 1989 *Comput. Phys. Commun.* **54** 391–407